

## Evaluation of the Effect for Liquefaction Strength and Deformation Characteristic by the Initial Shear Stress

K. Wakinaka<sup>1</sup>, S. Yasuda<sup>2</sup>, K. Ishikawa<sup>3</sup>,  
Y. Kitamura<sup>4</sup>, K. Oka<sup>5</sup>, R. Maruyama<sup>6</sup>

### ABSTRACT

Many cases of structural damage have been reported, which was caused by liquefaction under the structures such as river embankment. Under the structures, such as river embankment, the ground receives shear stress, besides vertical and/or horizontal anisotropic stress and initial shear stress. In this study, we conducted cyclic torsional shear tests in order to estimate the effect of the liquefaction strength and the deformation characteristic by the initial shear stress. The results showed that there were remarkable differences between the liquefaction strength and the deformation characteristic under different initial stress states. This results also led to the suggestion that it is important to evaluate appropriately the effect of initial shear stress when we estimate the liquefaction-related damages of the structures affected by initial shear stress.

### Introduction

Many structures such as river embankments received extensive damage by the liquefaction caused by the 2011 off the Pacific coast of Tohoku Earthquake on March 11, 2011. Many damage, which were assumingly caused by liquefaction of foundation ground, occurred in river banks. Many other damage, which have not been considered as the levee body damage caused by earthquakes, also generated. Especially in the toe of slope of the liquefied levee body, an initial shear stress  $\tau_i$ , in addition to the state of the anisotropic stress to vertical-horizontal direction, act as shown in Figure 1. If liquefaction occurred in such a ground, the strain develops to the direction of initial shear stress, and it is likely to cause large-scale damage. In this study, we conducted cyclic torsional shear tests acting initial shear stress, in order to clarify the influence that the initial shear stress exerts on the liquefaction strength and the deformation characteristic. Furthermore, we conducted a case analysis of liquefaction of levee body of river bank, which reflects the outcome of the test on the numerical analysis.

---

<sup>1</sup>Researcher, Kota WAKINAKA, Engineering administration division, Kawasaki Geological Engineering co., Ltd, Mita 2-11-15, Minato-ku, Tokyo 108-8337, JAPAN, [wakinakak@kge.co.jp](mailto:wakinakak@kge.co.jp)

<sup>2</sup>Professor, Susumu YASUDA, Dept of Civil and Environmental Engineering, Tokyo Denki University, Hatoyama, Hiki-gun, Saitama 350-0394, JAPAN, [yasuda@g.dendai.ac.jp](mailto:yasuda@g.dendai.ac.jp)

<sup>3</sup>Assistant professor, Keisuke ISHIKAWA, Dept of Civil and Environmental Engineering, Tokyo Denki University, Hatoyama, Hikigun, Saitama 350-0394, JAPAN, [ishikawa@g.dendai.ac.jp](mailto:ishikawa@g.dendai.ac.jp)

<sup>4</sup>Graduate student, Yui KITAMURA, Dept of Civil and Environmental Engineering, Tokyo Denki University, Hatoyama, Hikigun, Saitama 350-0394, JAPAN, [14rmg04@g.dendai.ac.jp](mailto:14rmg04@g.dendai.ac.jp)

<sup>5</sup>Undergraduate student, Kenichi OKA, Dept of Civil and Environmental Engineering, Tokyo Denki University, Hatoyama, Hikigun, Saitama 350-0394, JAPAN, [11rg018@g.dendai.ac.jp](mailto:11rg018@g.dendai.ac.jp)

<sup>6</sup>Undergraduate student, Ryosuke MARUYAMA, Dept of Civil and Environmental Engineering, Tokyo Denki University, Hatoyama, Hikigun, Saitama 350-0394, JAPAN, [11rg092@g.dendai.ac.jp](mailto:11rg092@g.dendai.ac.jp)

Table 1. Physical properties of Toyoura standard sand.

Physical properties of Toyoura standard sand			
Soil particles density $\rho_s$ (g/cm <sup>3</sup> )	2.65	Fine fraction content F <sub>c</sub> (%)	0
Maximum void ratio e <sub>max</sub>	0.604	Particle size 50% D <sub>50</sub> (mm)	0.261
Minimum void ratio e <sub>min</sub>	0.973	Particle size 20% D <sub>20</sub>	0.152

### Test methodology

Toyouira Standard Sand was used for the test (Table 1). Test pieces were stuffed with the sand to be a prescribed relative density. Target relative density of test pieces were;  $Dr=0\%$ , 30%, 50%, 70%. The initial shear stress is indicated as  $\alpha=\tau_i/\sigma_c$  which was adopted a ratio to effective confining pressure. In this test, we examined it at 5 stages of the initial shear stress ratio;  $\alpha=0-0.4$ . Under the condition of  $Dr=0\%$ , the test piece was destroyed by a strong initial shear stress ratio. Therefore, we tested it under the condition of  $\alpha=0$  and 0.1. The list of test conditions is shown in Table 2.

Under  $Dr=30\%-70\%$  conditions, test pieces were made by air pluviation method. Under  $Dr=0\%$  condition, air pluviation method was not suitable because test pieces were need to be loose fill. Therefore, the test piece was made with mixed breaking ice and sand. The test piece were midair cylinder type with outside diameter 10cm, inside diameter 6cm, height 10cm. Isotropic consolidation under effective confining pressure  $\sigma_c=20\text{kPa}$  was pressed, and a prescribed initial shear stress  $\tau_i$  was added with drained condition. After confirming that the excess pore pressure caused by the initial shear stress has completely disappeared, the cyclic loading was executed with sine wave after becoming the un-drained state by the initial shear stress. The number of cycles was 20 times at all test pieces. As shown in figure 2, liquefaction strength ratio  $R_L$  was defined from the cyclic shear stress ratio and the maximum shear strain. After the cyclic loading, in order to understand the deformation characteristic after liquefaction, a monotonic loading test was executed with pressing the initial shear stress. The monotonic loading test was performed by the strain control method at a loading speed of 10% per minute.

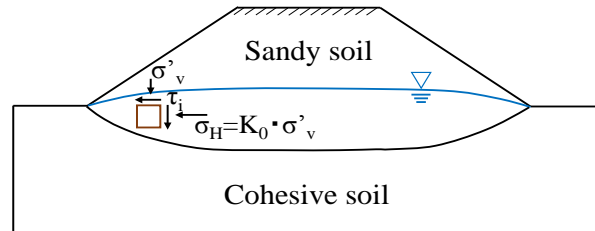


Figure 1. Initial shear stress in levee body liquefaction layer

Table 2. Test condition list

Relative density Dr(%)	Initial shear stress ratio $\alpha$	Relative density Dr(%)	Initial shear stress ratio $\alpha$
70	0	30	0
	0.1		0.1
	0.2		0.2
	0.3		0.3
	0.4		0.4
50	0	0	0
	0.1		0.1
	0.2		
	0.3		
	0.4		

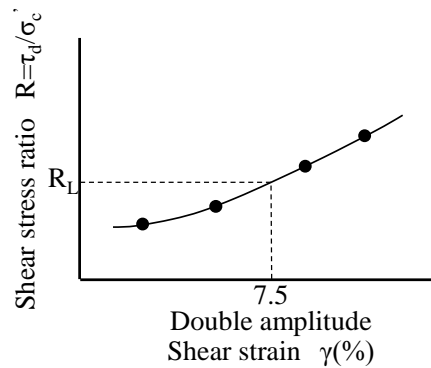


Figure 2. Definition of liquefaction strength ratio

### Test results

#### *Classification of failure morphology by the initial shear stress*

In the test with initial shear stress, the strain caused by cyclic loading exceeded to the direction of acting shear stresses. After the cyclic loading, it causes bigger residual stains due to the accumulation of the strain. Fracture morphologies by cyclic loading according to the initial shear stress were able to be divided into 4 main kinds. We describe here about four kinds failure morphologies.

#### (1)Cyclic failure ( $\alpha=0$ )

This failure morphology is a normal type under the condition without the initial shear stress. As shown in Figure 3-(a), the stress by cyclic loading acts on both positive and negative directions, and in accordance with this action, the strain occurs on the same direction with the stress. The amount of stress-strain roughly agrees with in both positive and negative directions. This is called the cyclic failure.

#### (2)Stress reverse cyclic failure ( $\alpha < R_d$ )

Stress reverse cyclic failure is a condition of the test with lower initial shear stress ratio than cyclic shear stress ratio. As shown in Figure 3-(b), the stress acts largely to the positive direction by the influence of the initial shear stress. Consequently, the strain indicates the dominant result

to positive direction. However, the cyclic shear stress ratio is higher than the initial shear stress ratio. It caused a reverse of the stress and strain, directing to the negative side as well. This is called the stress reverse cyclic failure.

(3) Stress non-reverse cyclic failure ( $\alpha > R_d$ )

Non stress reverse cyclic failure is a test condition that is examined with the initial shear stress ratio bigger than the cyclic shear stress ratio. As shown in Figure 3 (c), the results indicate that the initial shear stress is big and the stress occurs only to the positive direction. Consequently, the strain also occurs only to the positive direction. This is called the non-stress reverse cyclic failure.

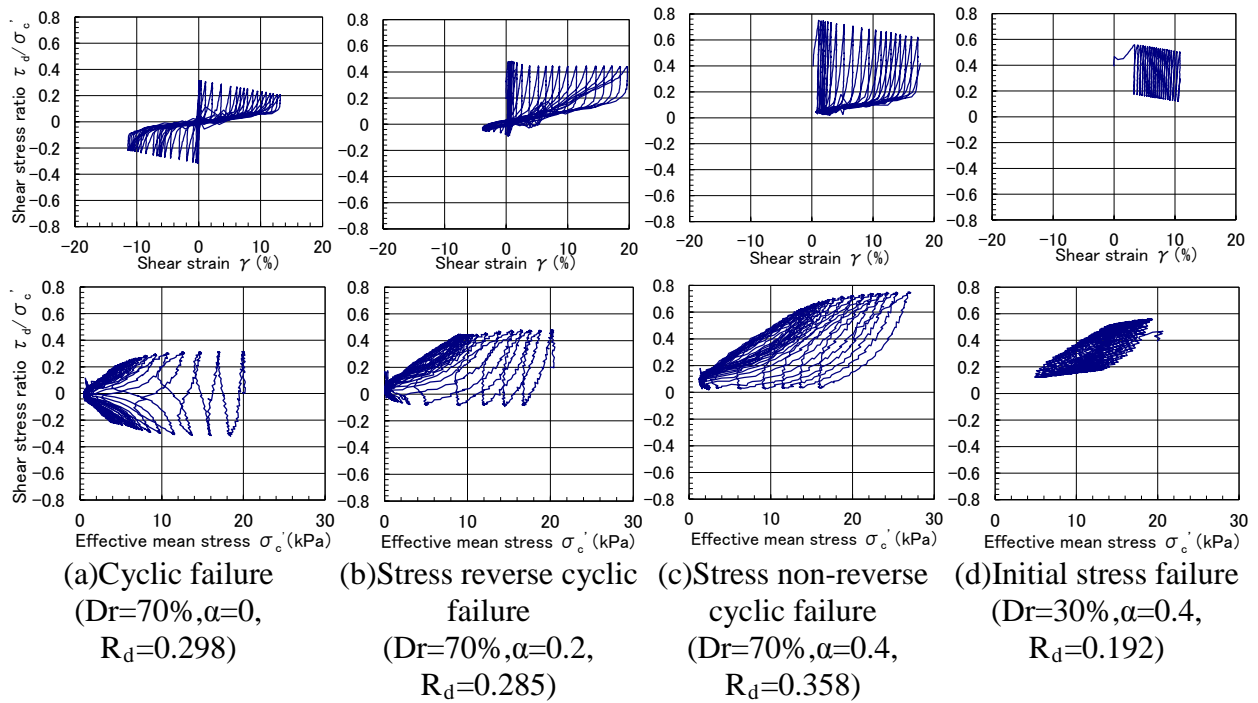


Figure 3. Classification of failure morphology

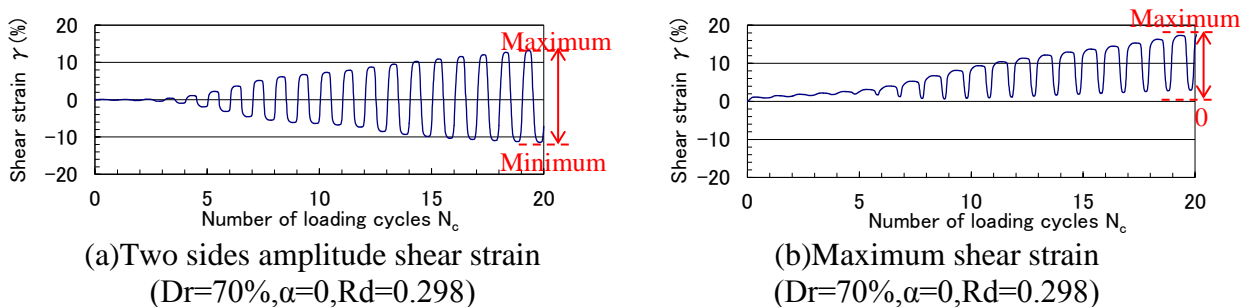


Figure 4. Definition method of strain

#### (4)Initial stress failure

The initial stress failure is the morphology that test piece destroys the first step of cyclic shear stress with a big strain of several percent under the strong initial shear stress on the loose test piece. And then, since the strain with cyclic shear stress continues to generate, the effective stress is never completely lost, and the strain causes over 7.5%. This is called the initial stress failure.

#### *Effect on liquefaction strength by the initial shear stress*

Liquefaction strength was calculated from the relation between cyclic shear stress ratio  $R_d$  at cyclic shearing and shear strain  $\gamma$  caused at cyclic shearing. As indicated in Figure 4-(a), the method of shear strain was defined as both side amplitude shear strain at the test without initial shear stress. As previous mentioned, the strain is directed to one side in the test with initial shear stress, therefore, as shown in Figure 4-(b), we defined it with maximum values of accumulation strain and amplitude shear strain.

The relation between cyclic shear stress ratio  $R_d$  and shear strain  $\gamma$  was plotted as shown in Figure 5. Liquefaction strength  $R_L$  obtained from the relation between shear stress ratio  $R_d$  and shear strain  $\gamma$  are shown in Figure 6. According to the test results of  $Dr=70\%$  and  $50\%$ , it is found that liquefaction strength is prone to decrease, compared to  $\alpha=0$  under the conditions categorized as stress reverse cyclic failure;  $Dr=70\%$ ,  $\alpha = 0.1$  or  $0.2$ ,  $Dr=50\%$ ,  $\alpha = 0.1$ . On the other hand, liquefaction strength is prone to increase, compared with  $\alpha=0$  under the condition of  $Dr=70\%$ ,  $\alpha=0.3, 0.4$  and  $Dr=50\%$ ,  $\alpha=0.3, 0.4$ , which is categorized as stress non reverse cyclic failure. It indicates that the initial shear stress has an influence on liquefaction strength not only by the strength of initial shear stress, but also by the application of stress reverse at the cyclic shear.

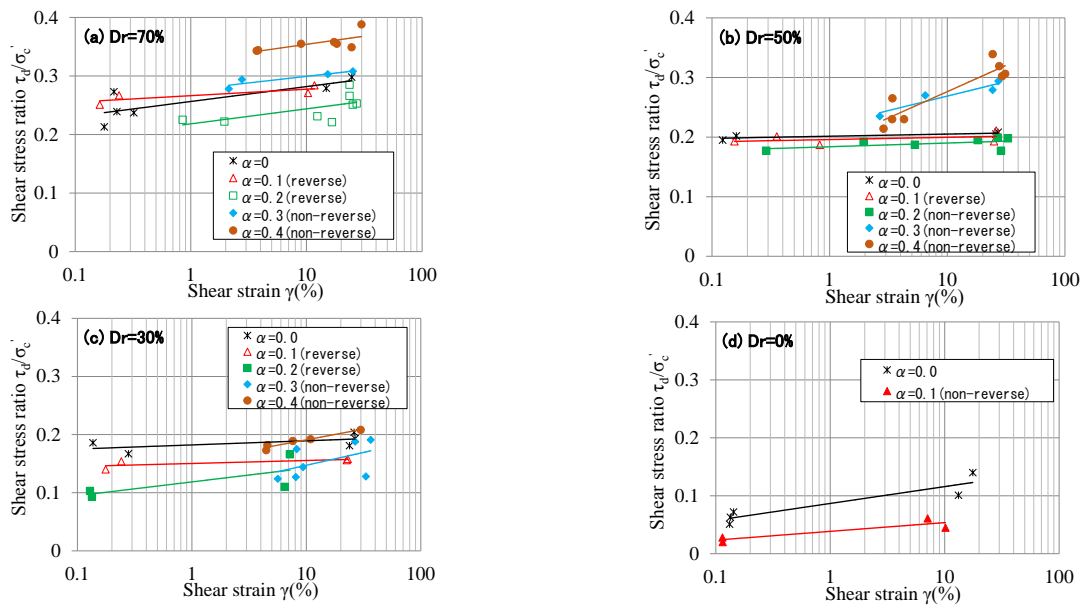


Figure 5. Relation between shear stress ratio and shear strain

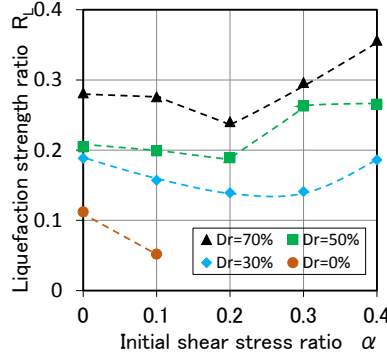


Figure 6. Relation between initial shear stress ratio and liquefaction strength ratio

On the other hand, the results of  $Dr=30\%$  shows that the liquefaction strength also decreases under  $\alpha=0.3, 0.4$  conditions which are categorized as stress reverse cyclic failure. Because these conditions are categorized into the initial stress failure out of fracture morphologies which described above, the failure causes the strain at first loading in which results in a large strain, and the liquefaction strength obtained from the relation between cyclic shear stress ratio  $R_d$  and shear strain  $\gamma$  decreases. The result of  $Dr=0\%$ ,  $\alpha = 0.1$  shows similar tendency as well.

#### *Effect of initial shear stress on deformation characteristic*

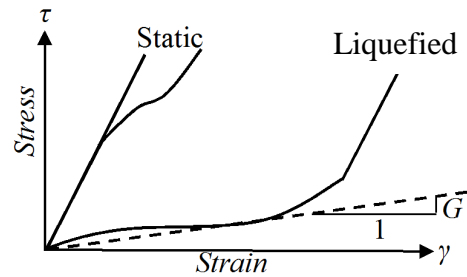
Stress-strain relations after liquefaction are divided into a small resistant region these modulus are very small, and a region after modulus recovery (Yasuda et al., 1999). Static monotonic loading test was conducted using test pieces after cyclic shear, and shear modulus of softened soil  $G_I$  was obtained by the gradient of tangent line in the small resistant region. In addition, the safety factor of liquefaction was defined as formula (1), in order to evaluate the liquefaction level of every test pieces quantitatively. Liquefaction strength ratio  $R_L$  indicates different values according to the initial shear stress. In this study,  $F_L$  is defined using liquefaction strength ratio  $R_{L\alpha=0}$  under the condition of non-active initial shear stress and cyclic shear stress ratio  $R_d$ .

$$F_L = R_{L\alpha=0} / R_d \quad \cdot \cdot \cdot (1)$$

The relations between  $G_I$  and  $F_L$  obtained by each examinations are shown in Figure 8. This explains that the deformation characteristic has changed as initial shear stress has been active.

Trend is thought to be similar to the liquefaction strength ratio  $R_L$ . Under the conditions of decreasing liquefaction strength ratio  $R_L$ , compared to  $\alpha=0$ , such as  $Dr=70\%$ ,  $\alpha=0.2$  and  $Dr=50\%$ ,  $\alpha=0.2$ , shear modulus of softened soil  $G_I$  tends to be decreased. Under the conditions of increasing liquefaction strength ratio  $R_L$ , compared to  $\alpha=0$ , such as  $Dr=70\%$ ,  $\alpha=0.3, 0.4$  and  $Dr=50\%$ ,  $\alpha=0.3, 0.4$ , shear modulus of softened soil  $G_I$  tends to be increased. As for  $Dr=70\%$ ,  $50\%$ ,  $\alpha=0.1$ , there was a little difference in both liquefaction strength ratio  $R_L$  and deformation characteristic. It is thought to be similar to  $Dr=30\%$ , under the conditions of  $\alpha=0.1 \sim 0.3$  declining liquefaction strength ratio  $R_L$  compared to  $\alpha=0$ . Thus, the reason why it has a correlation between the influence of the initial shear stress on the shear modulus  $G_I$  and the liquefaction strength ratio  $R_L$  is the defining method of the liquefaction factor  $F_L$ . As mentioned above, the liquefaction strength ratio  $R_L$  was adapted the value of  $\alpha=0$  with non-active initial shear stress in the definition of the liquefaction factor  $F_L$ . Under the condition of increasing the

liquefaction strength ratio  $R_L$ ,  $R_L$  is underestimated compared to its originality, and  $F_L$  is calculated small. On the other hand, under the condition of decreasing the liquefaction strength ratio  $R_L$ ,  $R_L$  is overestimated compared to its originality, and  $F_L$  is calculated big. Therefore, the correlation between shear modulus  $G_I$  in the small resistant region and liquefaction strength  $R_L$  was observed.



$G_I$ : Shear modulus of softened soil

Figure 7. Stress-strain relation of soil after liquefaction

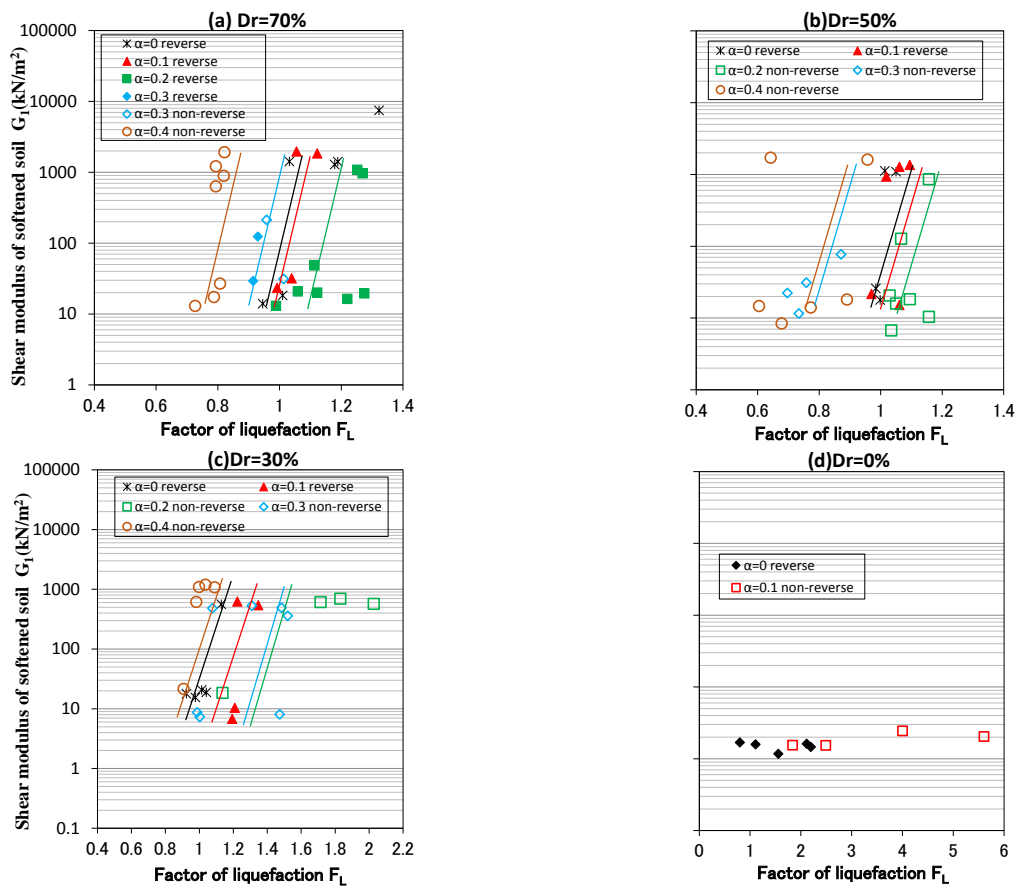


Figure 8. Relation between shear modulus of softened soil and factor of liquefaction

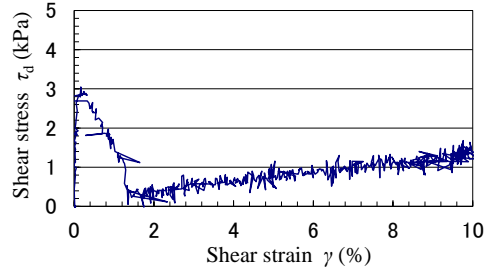


Figure 9. Monotonic loading test of  $D_r=0\%$

In the case of  $D_r=0\%$ , the shear modulus  $G_I$  in the small resistant region shows very small values, even though the liquefaction factor  $F_L$  indicates very big values. This is because, the test pieces were destructed immediately after starting the monotonic loading test, which inclined the gradient of the tangent, and  $G_I$  shows very small values. Stress-strain relation of the monotonic loading test of  $D_r=0\%$  is shown in Figure 9.

### Numerical analysis considering influence of initial shear stress

#### *Numerical analysis methodology*

A residual deformation method called ALID developed by Yasuda et al., 1999 was applied for the analysis, which is the finite element method for analyzing the seismic residual deformation by self-weight after decreasing the stiffness of liquefied layer. Stress relief technique was applied for self-weight analysis by liquefaction. At this time, shear modulus of softened soil  $G_I$  is calculated from liquefaction strength ratio  $R_L$  and liquefaction factor  $F_L$ . In this analysis, shear modulus  $G_I$  in the small resistant region has been set according to initial shear stress shown in Figure 8 and horizontal shear stress ratio acting at initial stress analysis.

#### *Analysis object section*

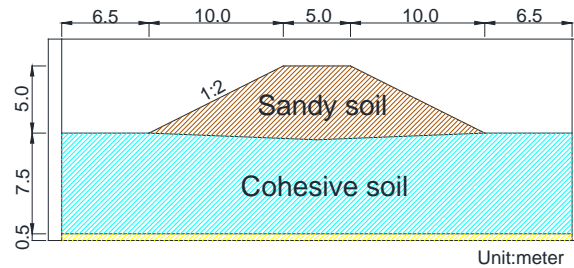


Figure 10. Model section of dynamic centrifuge tests

This analysis targeted the dynamic centrifuge model tests of the river bank by Public Works Research Institute (Tanimoto et al., 2012). This test was conducted on liquefaction of levee body with saturated sandy soil of lower part of levee body. The embankment shape is filled with 5.0m high and 20 percent grade of the slope. Figure 10 shows the model section of the centrifuge model test. In the test, the embankment crown subsided by approximately 1.3m and the levee body was destroyed on a large scale.



In the analysis, the saturated region in the lower part of the levee body was set as a liquefaction layer, and liquefaction strength ratio  $R_L$  was 0.19 from the test outcome. The analysis applied the condition of  $Dr=30\%$  of Figure 8-(c) from the value of  $R_L$ . The maximum acceleration of surface of the ground was 400gal from the test outcome.

### Numerical Analysis result

The analysis was performed in two ways in order to reveal the effect of the initial shear stress. The one is not to consider the effect of the initial shear stress, and the other is to consider it. Figure 11 shows the distribution of the horizontal shear stress ratio when the initial stress is analyzed. The horizontal shear stress ratio right under the levee crown indicates small value as less than 0.1. But, it is understood that big stresses such as 0.2-0.4 or more has acted as it moves to the toe of slope. This shows that some changes appear in the analytical result by analyzing it in consideration of the influence of initial shear stress.

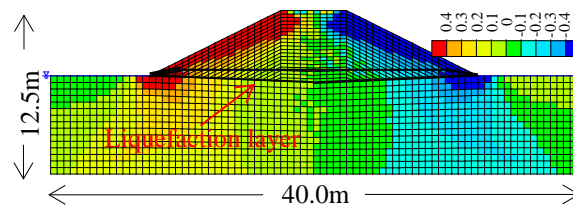


Figure 11. Distribution of horizontal shear stress ratio

Figure 12 shows the distribution of shear modulus  $G_1$  in the small resistant region from the analytical result. It is found that  $G_1$  of the element on which the initial shear stress acts, has decreased greatly from the distribution of  $G_1$ . Figure 13 shows the deformation chart of the outcome of the test and the analysis. It is found that the analytical result in which the influence of the initial shear stress is not considered, shows small deformation amount compared with the test results. It has been pointed out that liquefaction analysis of levee body tends to be underestimated, compared to actual deformation amount (Wakinaka et al., 2013). On the other hand, the analysis results which considered the influence of initial shear stress was able to, obtain closer amount of deformation by the test results, because the amount of the subsidence in the levee crown was increased due to the expansion of the slope as a bucking by the decline of  $G_1$  in the toe of the slope.

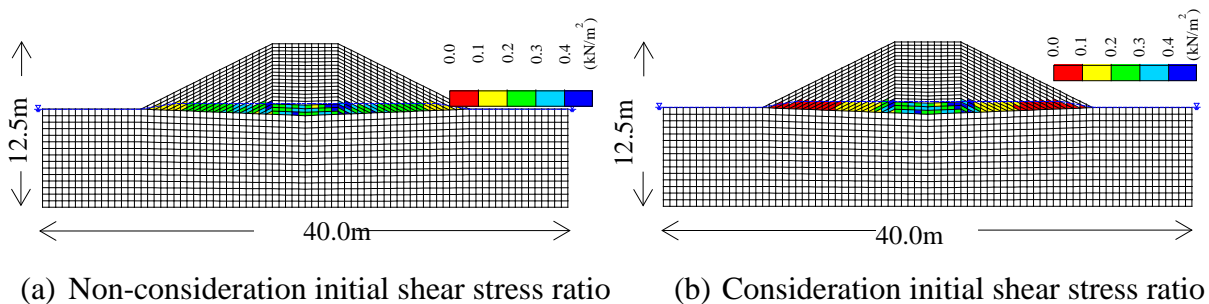


Figure 12. Distribution of shear rigidity of small region

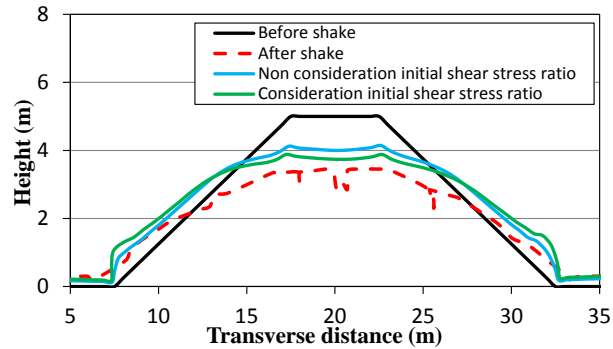


Figure 13. Comparison of deformation diagram

### Conclusions

The outcome of the cyclic torsional shear test with initial shear stress, revealed that the liquefaction strength ratio and the deformation characteristic after liquefaction were influenced by initial shear stress. The influence, on which initial shear stress put liquefaction strength ratio and deformation characteristic after liquefaction, differs from fracture morphologies. In stress reverse cyclic failure, we learnt that it tends to decrease liquefaction strength ratio and deformation characteristics. On the other hand, in stress non reverse cyclic failure, it tends to increase liquefaction strength ratio and deformation characteristics. Moreover, we understood that, in the initial stress failure with loose test pieces, it tends to decrease the liquefaction strength ratio and the deformation characteristic. In the liquefaction analysis of the levee body which its deformation amount was undervalued, the outcome of the analysis which considers the influence of initial shear stress enabled us to obtain the deformation amount which is closer to the actual value. In the next step, the authors intend to conduct the liquefaction analysis in the profile of river embankment damaged by earthquakes.

### References

- Tanimoto S, Hayashi H, Ishihara M, Masuyama H. Dynamic centrifuge tests on countermeasure against liquefaction of saturated bottom part of river embankment. *Geotechnical workshop* 71-89. 2012.
- Wakinaka k, Ishihara M, Sasaki T. Numerical analysis of due to liquefaction in levee body in the Great East Japan. *Geotechnical workshop* 1701-1702. 2013.
- Yasuda S, Yoshida N, Adachi K, Kiku H, Gose S, Masuda T. A simplified practical method for evaluating liquefaction-induced flow. *Journal of Japan Society of Civil Engineers* 71-89. 1999.